




## Article

# The Impact of El-Niño and La-Niña on the Pre-Monsoon Convective Systems over Eastern India

Rajesh Kumar Sahu<sup>1</sup>, Goutam Choudhury<sup>2</sup>, Naresh Krishna Vissa<sup>1</sup>, Bishma Tyagi<sup>1,\*</sup>  
and Sridhara Nayak<sup>3,\*</sup>

<sup>1</sup> Department of Earth and Atmospheric Sciences, National Institute of Technology, Rourkela 769008, India

<sup>2</sup> Leipzig Institute for Meteorology, Leipzig University, 04103 Leipzig, Germany

<sup>3</sup> Earth Science Center, Japan Meteorological Corporation, Osaka 530-0011, Japan

\* Correspondence: tyagib@nitrrkl.ac.in (B.T.); nayak.sridhara@n-kishou.co.jp (S.N.)

**Abstract:** El-Niño and La-Niña are believed to change the intensity and frequencies of extreme weather events globally. The present study aims to analyse the impact of El-Niño and La-Niña on the lightning activities of cloud systems and their associated precipitation and thermodynamic indices over the Eastern India regions (Odisha, Jharkhand, and West Bengal) during the pre-monsoon season (March–May). Eastern India receives catastrophic thunderstorm events during the pre-monsoon season. The results suggest that the number of lightning flashes was higher in the El-Niño years than in the La-Niña periods, which helps convective activities to be developed over the study region. The precipitation variations showed similar patterns during El-Niño and La-Niña periods, but the magnitudes were higher in the latter. Results from the analysis of thermodynamic indices show that, during the La-Niña phase, the convective available potential energy (CAPE), convective inhibition (CIN), severe weather threat index (SWEAT), humidity index (HI), and total totals index (TTI) values increased, while the cross total index (CTI) and K index (KI) decreased. In contrast, the vertical total index (VTI) and Boyden index (BI) values showed less significant changes in both El-Niño and La-Niña periods. The anomalies of flash rate densities over most parts of our domain were positive during the El-Niño years and negative during the La-Niña years. Precipitation anomalies had a higher positive magnitude during the La-Niña phase, but had spatial variability similar to the El-Niño phase. The anomalies of most of the thermodynamic indices also showed noticeable differences between El-Niño and La-Niña periods, except for the HI index. El-Niño periods showed higher lightning and increased values of associated thermodynamic indices over eastern India, indicating more pronounced convective systems.

**Keywords:** El-Niño; La-Niña; thermodynamic indices; precipitation; FRD



**Citation:** Sahu, R.K.; Choudhury, G.; Vissa, N.K.; Tyagi, B.; Nayak, S. The Impact of El-Niño and La-Niña on the Pre-Monsoon Convective Systems over Eastern India. *Atmosphere* **2022**, *13*, 1261. <https://doi.org/10.3390/atmos13081261>

Academic Editors: Zhiping Wen and Ioannis Charalampopoulos

Received: 28 June 2022

Accepted: 4 August 2022

Published: 9 August 2022

**Publisher's Note:** MDPI stays neutral with regard to jurisdictional claims in published maps and institutional affiliations.



**Copyright:** © 2022 by the authors. Licensee MDPI, Basel, Switzerland. This article is an open access article distributed under the terms and conditions of the Creative Commons Attribution (CC BY) license (<https://creativecommons.org/licenses/by/4.0/>).

## 1. Introduction

El-Niño and La-Niña are associated with El-Niño Southern Oscillations (ENSO), an ocean and atmospheric coupled phenomenon generally observed in the tropical Pacific Ocean. ENSO occurs due to irregular sea surface temperature (SST) and wind pattern changes. The warm and cold phases of ENSO are termed El-Niño and La-Niña, respectively [1]. The El-Niño period can last up to 9 to 12 months and can potentially destroy marine life during extreme conditions in the tropical Pacific Ocean [2]. During El-Niño, the SST changes drastically, switching convective activities from west to east in the tropical Pacific Ocean. During La-Niña, the SST reduces, facilitating the westward drift of wind stress. The climatic surroundings of the maritime continent and south-eastern China are heavily impacted by both El-Niño and La-Niña phases in the Asian sector. As a result, there is an unusual dispersal of rainfall and an increase in lightning flashes in that area [3,4]. El-Niño and La-Niña are also responsible for inter-annual lightning anomalies on regional and global scales [5].

El-Niño years are associated with warmer atmospheric conditions favourable for the generation of convective activities far eastward from the western Pacific Ocean. Many studies have reported lightning activities and associated storms during El-Niño and La-Niña over different parts of the globe [6–12]. An increase in the number of lightning flashes during El-Niño and a decrease during La-Niña periods over east Asia was revealed by Shinji et al. [11]. Kulkarni et al. [13] studied the association of thunderstorms during El-Niño over Indian land regions and suggested that the thunderstorm days decreased during the El-Niño periods. Moreover, Roy et al. [14] found the El-Niño and La-Niña years to be associated with drought and excess rainfall years, respectively. Saha et al. [15] analysed the spatial and temporal lightning variability associated with convection during El-Niño and La-Niña episodes for the years 1997–2013 over the whole Indian subcontinent for all the seasons. The total lightning flash rate density study using the TRMM-LIS data has been carried out in many regions of the globe, including Northeast Brazil [16], Northern Alabama [17], Southwest Iran [18], and India [19]. As per the findings of Saha et al. [15], El-Niño periods are associated with reduced convective activities and enhanced lightning activities over the Indian region compared to La-Niña.

The pre-monsoon season over eastern India is usually associated with catastrophic thunderstorms [20,21]. These thunderstorms, aided by an immense moisture supply from the Bay of Bengal, are accompanied by severe rainfall, wind speed, and lightning [22,23]. They are not only responsible for the deaths of numerous human beings and livestock but also for the destruction of agricultural crops [24–26]. Since thermodynamic indices for thunderstorm analysis are known to be important, established thermodynamic indices are already widely utilized by researchers over the region, but many new indices have also been developed for eastern India [27–29]. Given the severity of thunderstorms associated with the region [30], a detailed analysis of the variability of thermodynamic indices during the El-Niño and La-Niña phases is still missing for most parts of India. Thermodynamic indices are widely used as a valuable tool for predicting thunderstorms [31,32]. The persistent rise in CAPE over India was observed by Murugavel et al. [33]. Chakraborty et al. [34] discussed the thermodynamic instability constraints, large-scale dynamics, and a drop in upper-tropospheric temperatures for the period 1998–2014. Previous studies have found that the lightning activities over the Indian region are modulated by the El-Niño and La-Niña phases. As the lightning activities change, the thunderstorm frequencies and intensities also evolve, thereby changing the thermodynamic indices.

As the thunderstorms during the pre-monsoon months are catastrophic and their prediction and assessment are important for safeguarding the lives and property in the region, it will be worth seeing if the ENSO is changing the frequency or intensity of these thunderstorm events. The present work focuses explicitly on eastern India during the pre-monsoon season, emphasising the thermodynamic indices of spatial variability for the last seventeen years (1998–2014). We also use the lightning and precipitation maps over the selected region to analyse the severity of convective activities. As the changing climate is impacting the thunderstorms over the region during the pre-monsoon season [35,36], the present study focuses on identifying the variations of (i) the lightning and associated rainfall and (ii) the strength of thermodynamic indices during El-Niño and La-Niña periods over eastern India during the pre-monsoon season.

## 2. Study Area, Data, and Methodology

The study area for the present study is eastern India: Odisha, Jharkhand, and West Bengal states. Odisha is in the Eastern Ghats regions of the Deccan plateau, while Jharkhand is situated over the Chhotanagpur region and West Bengal in the Indo-Gangetic plain. These three states are in the humid subtropical area with gentle winter from November to February, scorching summer from March to June, and monsoon from July to October with substantial rainfall [36]. Most of the interior parts of these states have extremely hot and dry climates during summer and winter; nonetheless, the entire area receives substantial rainfall during the monsoon season. This area experiences more lightning and thunderstorms with

higher frequency and intensity during the pre-monsoon season. Figure 1 depicts the study domain for the present study: Odisha, Jharkhand, and West Bengal.

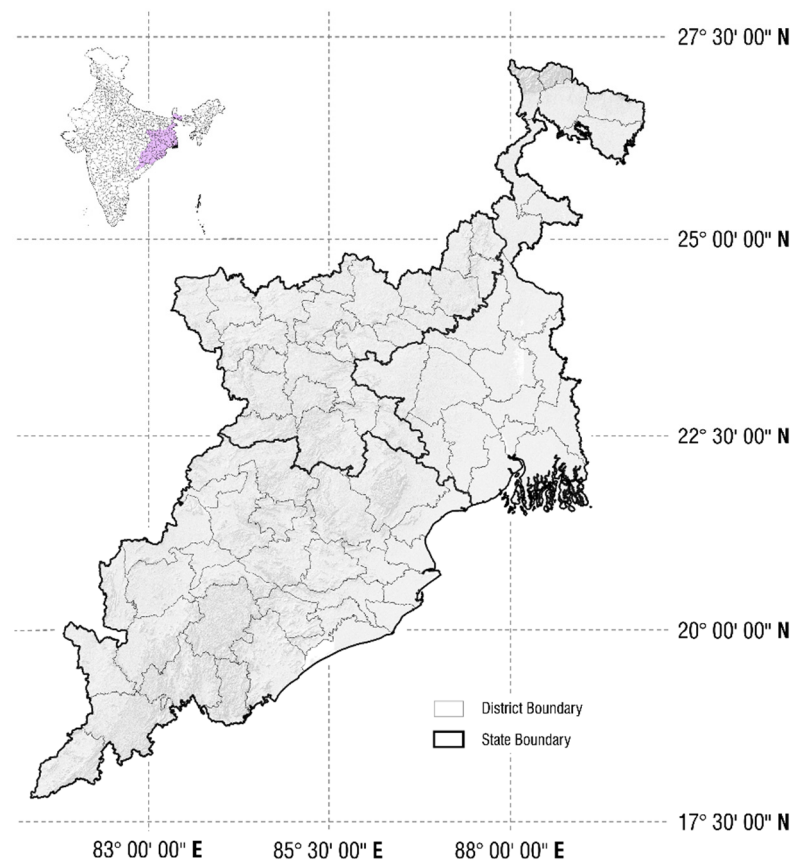


**Figure 1.** Study area of Eastern India which covers Odisha, Jharkhand and West Bengal.

The spatial variation of the thermodynamic indices over this study domain was studied for the pre-monsoon season (March–May) of 1998–2014 using the monthly mean ERA5: European Center for Medium-Range Weather Forecast (ECMWF) reanalysis data 5. The details of ERA5 data may be obtained from Hersbach and Dee [37]. The thermodynamic indices used in this study were the Boyden index (BI), cross total index (CTI), convective available potential energy (CAPE), convective inhibition (CIN), humidity index (HI), K index (KI), total totals index (TTI), severe weather threat index (SWEAT), and vertical total index (VTI). These thermodynamic indices are defined by Kunz [31] and Haklander and Delden [32].

The geographic locations of the lightning flashes were obtained from the satellite Tropical Rainfall Measuring Mission with the lightning imaging sensor (TRMM-LIS) for the available pre-monsoon period 1998–2014 (<https://ghrc.nsstc.nasa.gov/hydro/#/details?ds=lislip> (accessed on 4 September 2021)). The Tropical Rainfall Measuring Mission (TRMM) satellite circles the Earth at 350 kilometres above sea level between 35° N and 35° S at a rate of 16 orbits per day, providing the lightning observations used in this study [38]. With flash detection efficiencies of 73.11% and 93.4%, these LISs can detect cloud-to-ground and intra-cloud discharges, whether at day or night [39]. For the present study, the corresponding flash rate density was estimated within a uniform  $0.5^\circ \times 0.5^\circ$  (lat  $\times$  lon) grid by calculating the number of flashes per unit area of the grid cell per year ( $\text{km}^{-2} \text{yr}^{-1}$ ), following the methodology given in Cecil et al. [40]. The details of the lightning imaging sensors are available from Christian et al. [38], Williams et al. [41], and Bond et al. [42]. We also used TRMM/3B43 V7 L3 monthly mean rainfall data for the pre-monsoon period obtained from the Tropical Rainfall Measuring Mission satellite with  $0.25^\circ \times 0.25^\circ$  (lat  $\times$  lon) resolutions ([https://disc.gsfc.nasa.gov/datasets/TRMM\\_3B43\\_7/summary?keywords=TRMM](https://disc.gsfc.nasa.gov/datasets/TRMM_3B43_7/summary?keywords=TRMM)

(accessed on 6 September 2021)). The details of the El-Niño and La-Niña years were collected from the National Oceanic Atmospheric Administration’s Climate Prediction Center (NOAA/CPC) of the National Weather Service ([https://origin.cpc.ncep.noaa.gov/products/analysis\\_monitoring/ensostuff/ONI\\_v5.php](https://origin.cpc.ncep.noaa.gov/products/analysis_monitoring/ensostuff/ONI_v5.php) (accessed on 10 September 2021)). The El-Niño years considered in our study were in consecutive monthly periods: 1998, 2006, and 2010, and the La-Niña years were 1999, 2000, 2008, 2009, 2011 and 2012 during pre-monsoon months (March–May). In other years, pre-monsoon months were termed neutral years.

The analysis employed anomaly calculations for lightning, rainfall, and thermodynamic indices. The use of anomaly calculations brings out minute changes in reference to different experiments/situations over a particular region for a dataset [43]. The anomalies were calculated by differencing the El-Niño and La-Niña years with the whole data period, i.e., 1998–2014.

### 3. Results and Discussion

#### 3.1. Lightning Activity Difference in El-Niño and La-Niña

We analyse the variations in the flash rate density (FRD, flashes) and rainfall for the El-Niño episodes of 1998, 2006, and 2010 and for the La-Niña episodes of 1999, 2000, 2008, 2009, 2011, and 2012 during the pre-monsoon months. The FRD variations during the El-Niño periods are shown in Figure 2a, the La-Niña periods in Figure 2b and the total FRD in Figure 2c. The FRD analysis (Figure 2c) shows that the study regions have high flash rates over a few areas: southern and northern Odisha, central Jharkhand, and northern parts of West Bengal. The FRD was more prominent during the El-Niño period (Figure 2a). The highest FRD was observed over the north, central, and west regions of West Bengal, whereas for Odisha, high values were recorded over the southern, central, and northern regions. The observed high FRD regions of central Jharkhand during the total period (Figure 2c) shifted to the southern and north-eastern parts of Jharkhand during the El-Niño period. Although the higher FRD regions were active even during the La-Niña years, the intensity decreased over all the significant areas, except the central parts of Jharkhand (Figure 2b), where the FRD was highest (>180). The anomaly plots of FRD (from El-Niño, La-Niña, and average plots) supported the observation of high/less FRD during El-Niño/La-Niña years (Figure 3a,b).

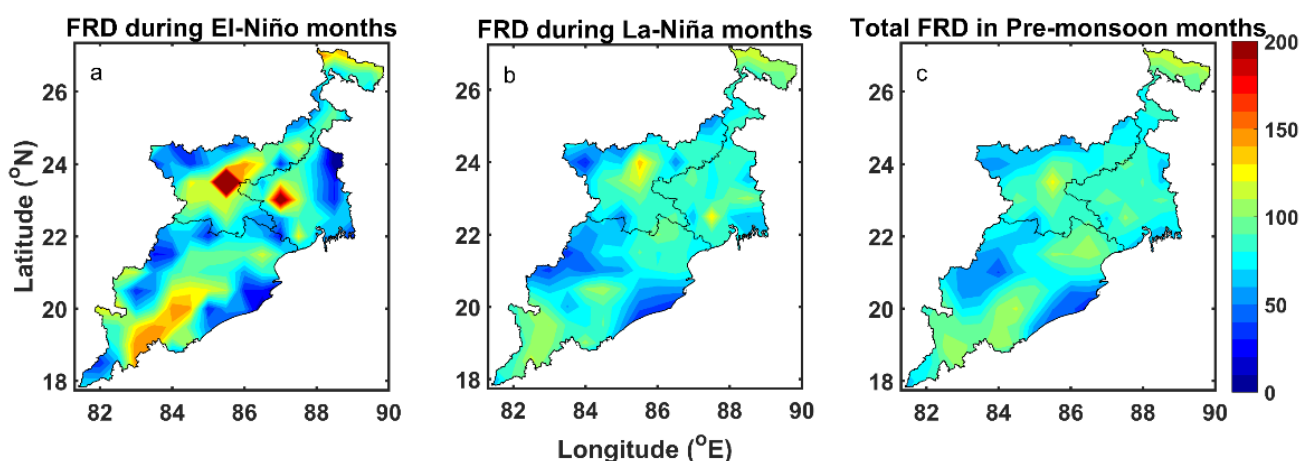
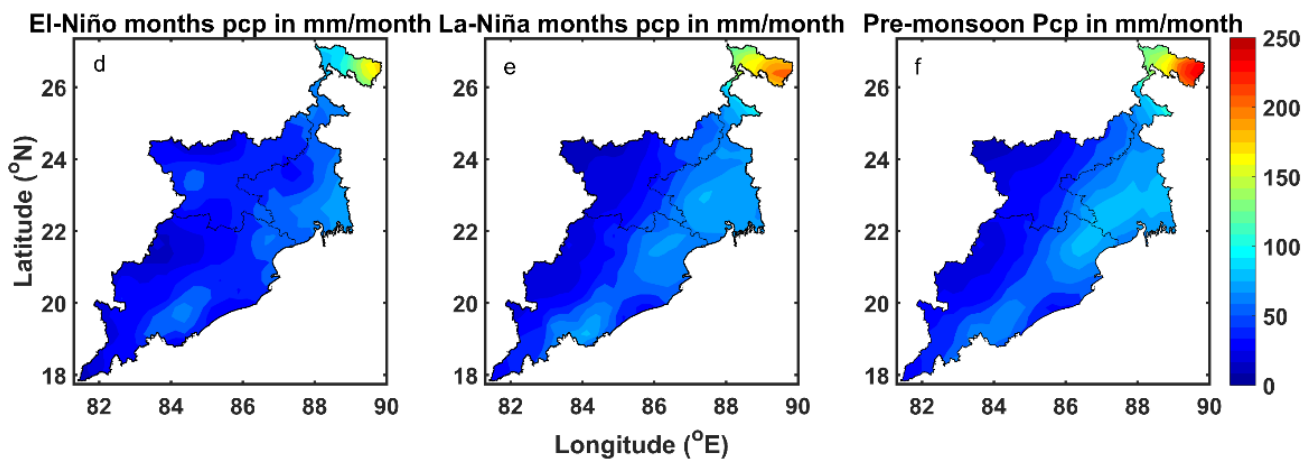
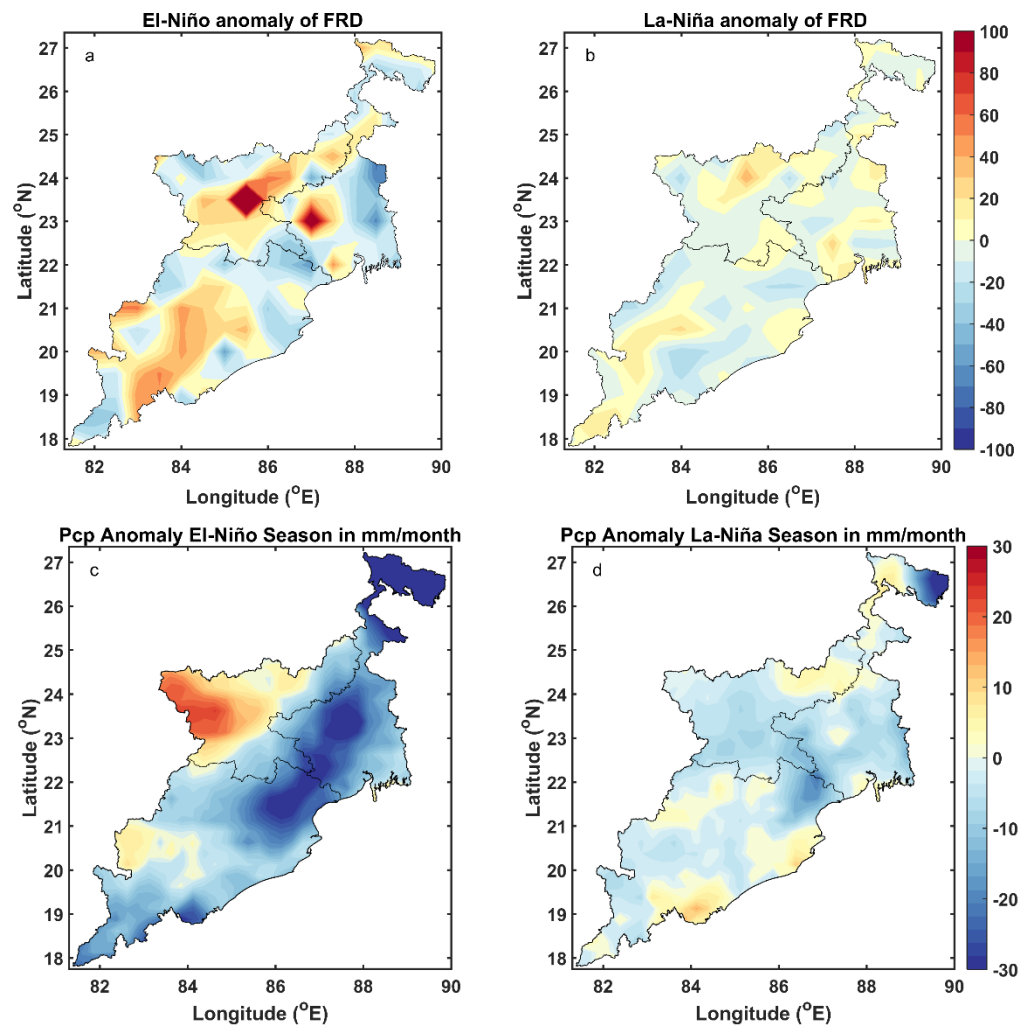


Figure 2. Cont.



**Figure 2.** FRD variations during (a) El-Niño, (b) La-Niña, and (c) the total FRD, and accumulated precipitation variations during (d) El-Niño, (e) La-Niña, and (f) total pre-monsoon precipitation from 1998–2014.



**Figure 3.** FRD anomalies (a) El-Niño, (b) La-Niña (upper row) and precipitation anomalies (c) El-Niño, (d) La-Niña (bottom row) during pre-monsoon season from 1998–2014.



### 3.2. Precipitation Variations during El-Niño and La-Niña Episodes and Their Anomaly

The accumulated precipitation variations during El-Niño (Figure 2d), La-Niña (Figure 2e), and total El-Niño/La-Niña years (Figure 2f) per season during pre-monsoon months are shown in Figure 2. The overall rainfall patterns were similar for both El-Niño and La-Niña periods, where the highest intensity was over the northern (Darjeeling, Jalpaiguri, Cooch Behar) West Bengal region, with higher precipitation over northern (Mayurbhanj, Kendujhar, Balasore) Odisha and some parts of western (West Medinipur, Bankura) and north (Darjeeling, Jalpaiguri, Cooch Behar) West Bengal regions. The seasonal precipitation anomaly for El-Niño (Figure 3c) and La-Niña (Figure 3d) for the study period during pre-monsoon months was plotted. For the El-Niño years (Figure 3c), except for a few regions of western Odisha (Nuapada, Balangir, Kalahandi), all other regions showed negative anomalies. In Jharkhand, except for the north-eastern, southern, and south-eastern parts, the other regions showed a positive anomaly. However, for West Bengal, all the regions showed a negative precipitation anomaly. The highest negative anomaly was observed over the northern Odisha (Mayurbhanj, Balasore, and Kendujhar districts) and western (Bankura, Purulia, West Medinipur, Jhargram) and northern parts (Darjeeling, Jalpaiguri, Cooch Behar, Alipurduar) of West Bengal. In the case of La-Niña, a similar precipitation pattern was visible with a higher magnitude. The anomaly plots show considerable precipitation (Figure 3d) in some parts of eastern Indian states. Though the precipitation difference in both El-Niño and La-Niña periods was not noteworthy, the region experienced higher precipitation during La-Niña.

### 3.3. Thermodynamic Indices Variations during El-Niño and La-Niña Episodes and Their Anomalies

The spatial variation of thermodynamic indices is useful in understanding the variability of thermodynamic indices over the region, especially with respect to convective events [44,45]. To analyse the CAPE, CIN, and SWEAT variability, we made three groups: El-Niño years, La-Niña years, and neutral years for El-Niño/La-Niña period shown in Figure 4. During all three periods, coastal districts have higher CAPE values, exceeding  $>3500$  J/Kg in some coastal Odisha and West Bengal districts. The CAPE values decrease from coast to inland areas, indicating the role of the Bay of Bengal in providing moisture supply and creating a conducive environment over the coastal region. To visibly understand the spatial variations during El-Niño/La-Niña periods, we analysed the anomalies of different thermodynamic indices during El-Niño and La-Niña periods. In Figure 4d,e, the CIN values were shown to increase i.e.,  $>600$  J/Kg in the coastal parts of Odisha, West Bengal, and some of the parts of Jharkhand region during the El-Niño phase, but the magnitude of CIN was less than the La-Niña and neutral years. Similarly, as shown in Figure 4g-i, the SWEAT values increased, i.e.,  $>180$  in most of the period, but the values were somewhat higher for La-Niña than El-Niño.

Figure 5 shows the anomalies of CAPE, CIN, and SWEAT during the El-Niño and La-Niña period from 1998 to 2014. During El-Niño, except for the Nuapada and Balangir districts of Odisha, all other parts showed a negative anomaly of CAPE (Figure 5a). Except for northern West Bengal districts (Darjeeling, Kalimpong, and parts of Jalpaiguri), all other regions showed a negative anomaly of CAPE. In Jharkhand, except for parts of north-eastern and south-eastern Jharkhand districts, other regions showed a positive anomaly during the El-Niño phase. The negative anomaly values, indicating reduced CAPE values over the Odisha, West Bengal, and north-eastern and south-eastern parts of Jharkhand during El-Niño, persisted even during the La-Niña period. However, most of the eastern India region showed a negative anomaly, except some parts of the western West Bengal district and parts of north-eastern Jharkhand, which showed a slight positive anomaly value during La-Niña (Figure 5b). The spatial variability shows that CAPE values were lower over Odisha and West Bengal during the El-Niño and La-Niña years, with comparatively higher values over Jharkhand.

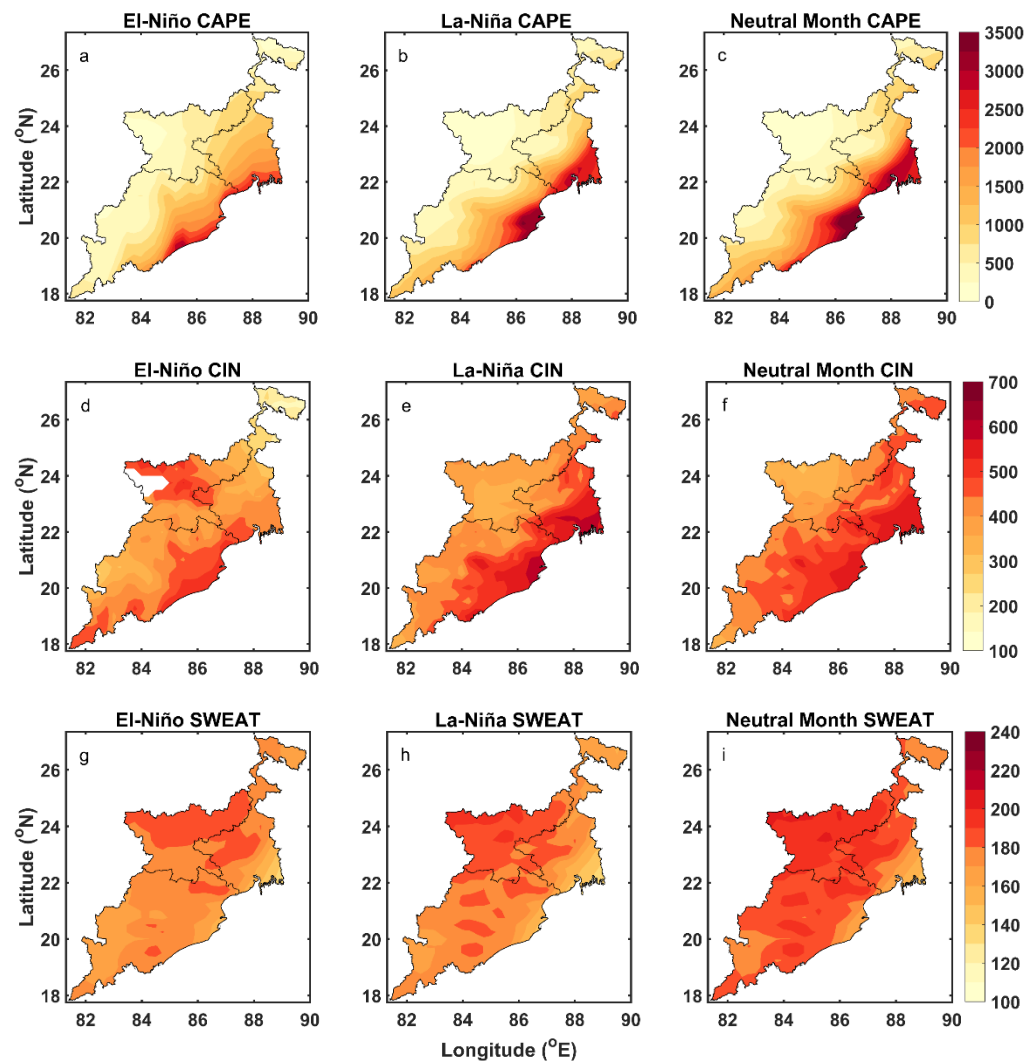


**Figure 4.** Variation of CAPE (a) El-Niño, (b) La-Niña and (c) Neutral months (first row), CIN (d) El-Niño, (e) La-Niña and (f) Neutral months (second row), and SWEAT (g) El-Niño, (h) La-Niña and (i) Neutral months (third row) during the pre-monsoon season from 1998–2014.

The CIN values were higher during the La-Niña period. Odisha and West Bengal showed higher CIN values in the La-Niña years, with the highest values observed in the coastal areas of Odisha (~500–650 J/Kg), West Bengal (~550–650 J/Kg), and northern parts of Odisha. Over Jharkhand, the CIN values were higher during La-Niña (~350–500 J/Kg), but the magnitude of the CIN values was smaller than Odisha and West Bengal. The CIN anomalies during the El-Niño (Figure 5c) and La-Niña (Figure 5d) periods from 1998 to 2014 were also able to bring out the differences in spatial variations.

The spatial variability of CIN differed not only over coastal areas, but also in the inland districts of Odisha, sharing a border with other states (mainly western and northern regions) and over northwest Bengal during El-Niño and La-Niña. However, the magnitudes were slightly higher during the La-Niña period. During the El-Niño period (Figure 5c), most of the parts of Odisha, along with West Bengal, showed negative CIN anomalies except for the western districts (Nabarangpur, Nuapada, Kalahandi) of Odisha and northern and western districts (Bankura; Malda; Darjeeling; Kalimpong, and parts of Jalpaiguri, Uttar, and Dakshin Dinajpur) of West Bengal. A slightly positive anomaly was observed over the Godda district of Jharkhand. During the La-Niña period, most of the areas of West Bengal showed positive anomalies. The exceptions were some parts of the western (Purulia, Bankura, Paschim Bardhaman, Birbhum districts) and northern (Darjeeling, Cooch Behar, Kalimpong, Jalpaiguri, Alipurduar, Malda Uttar and Dakshin Dinajpur districts)

regions, which showed negative anomalies (Figure 5d). Except for western (some parts of Sundergarh, Jharsuguda, Bargarh, Sambalpur, Kalahandi, Nabarangpur, Nuapada and Balangir), northern (Kendujhar), and parts of southern (Malkangiri, Koraput) Odisha, all other regions showed positive CIN anomalies during La-Niña. During El-Niño, almost all the areas of Jharkhand showed negative CIN anomalies, whereas during La- Niña, except northern (Koderma, Hazaribagh, Chatra districts) and western (Palamu, Garhwa, Latehar districts) Jharkhand regions, other parts are showed negative CIN anomalies.

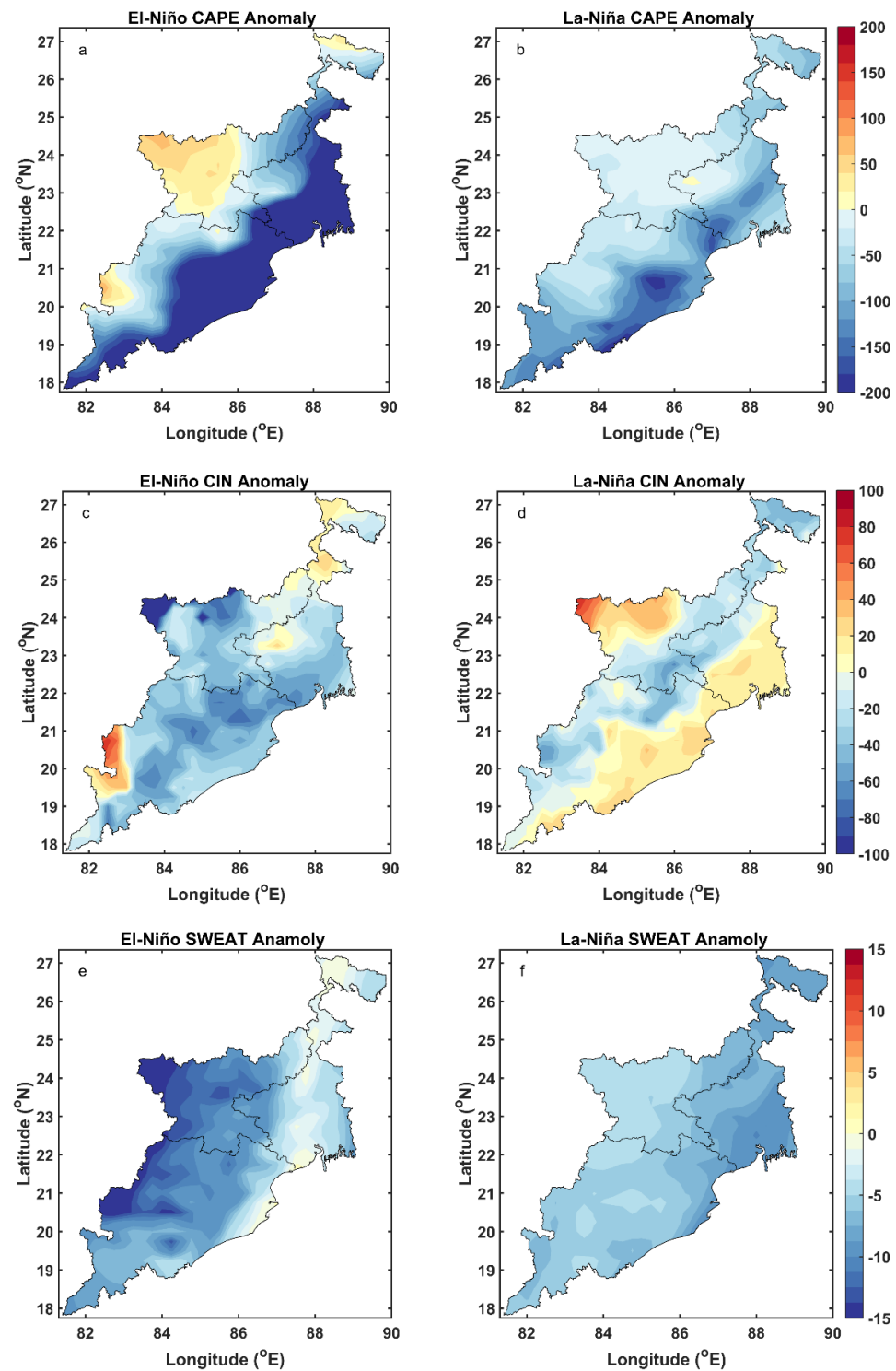


**Figure 5.** Anomalies of CAPE (a) El-Niño, (b) La-Niña (first row) CIN (c) El-Niño, (d) La-Niña (second row), and SWEAT (e) El-Niño, (f) La-Niña (third row) during the pre-monsoon season.



SWEAT values were generally high over the region [35,36]. The spatial variations of SWEAT during El-Niño, La-Niña, and neutral El-Niño/La-Niña episodes confirmed this spatial pattern of high values, with lower values in coastal regions and increasing values inland. However, the values during the El-Niño spells were relatively low over eastern India, as evident from SWEAT anomalies during El-Niño (Figure 4e) and La-Niña (Figure 4f). During both the El-Niño and La-Niña periods, almost all the parts showed a negative SWEAT anomaly. During the El-Niño periods, most of the parts of eastern India showed a negative SWEAT anomaly, but the magnitude was less over West Bengal compared to the other two states. During the La-Niña periods, the negative SWEAT anomalies were less than those of El-Niño over most parts of eastern India.

We also analysed other thermodynamic indices (CTI, TTI, VTI, KI, BI, HI) during the El-Niño, La-Niña, and neutral El-Niño/La-Niña periods in the pre-monsoon seasons from 1998 to 2014, as shown in Figures 6–8. The CTI values were higher during the El-Niño periods. Apart from CTI, all other indices showed higher values during the La-Niña periods. HI values showed a clear difference between El-Niño and La-Niña and the values were higher during the La-Niña periods (Figures 6–8). Figure 9 shows the CTI (a), VTI (b), TTI (c), BI (d), HI (e), and KI (f) anomalies during the El-Niño years, and Figure 10 shows the CTI (a), VTI (b), TTI (c), BI (d), HI (e), and KI (f) anomalies during the La-Niña years from 1998 to 2014. Except for the HI index, all the other indices showed negative anomalies during El-Niño. The HI anomaly clearly differentiates the El-Niño and La-Niña periods over eastern India, with a positive anomaly during the La-Niña for the whole eastern India region (Figure 10). VTI and BI also showed slightly positive anomalies during the La-Niña periods, whereas during El-Niño, a negative anomaly was shown for most of the parts of eastern India. During El-Niño, HI values show negative anomalies, except for the parts of coastal (Ganjam, Puri, Jagatsinghpur, Kendrapara, Balasore) and southern (Malkangiri, Koraput) districts of Odisha, as well as coastal (Purba Medinipur, South 24 Parganas, Howrah), eastern (North 24 Parganas, Nadia, Murshidabad, Hooghly, parts of Purba Bardhaman and Malda), and some parts of northern (Cooch Behar, Alipurduar) districts of West Bengal, which showed positive anomalies.

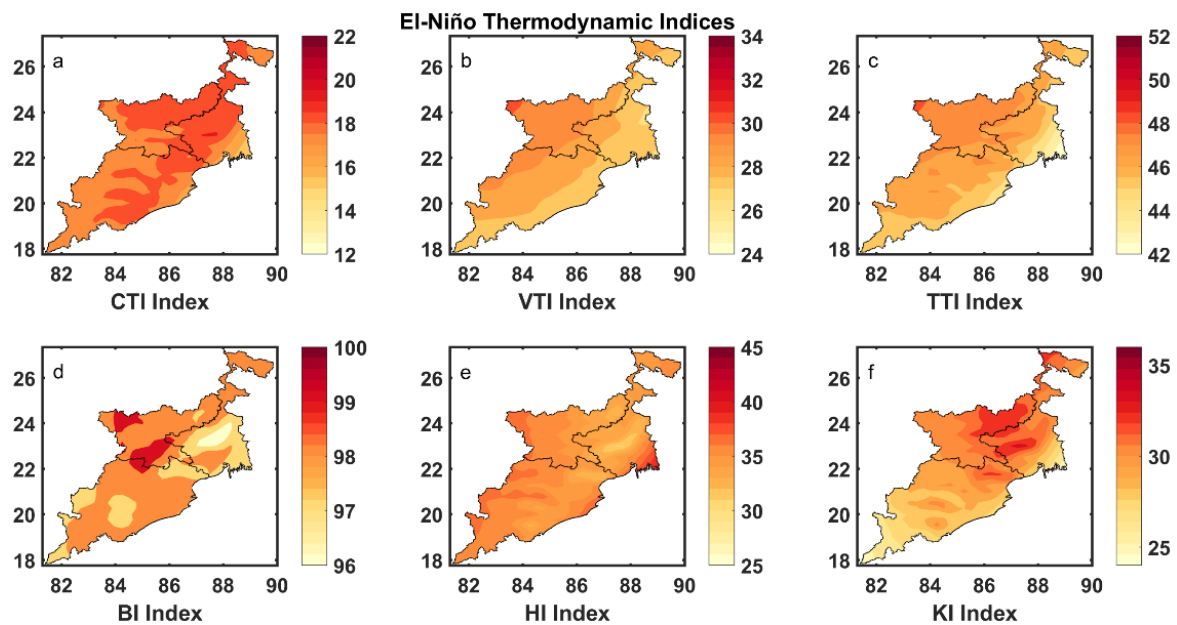


Figure 6. CTI (a), VTI (b), TTI (c), BI (d), HI (e), KI (f) variations during El-Niño years from 1998 to 2014.

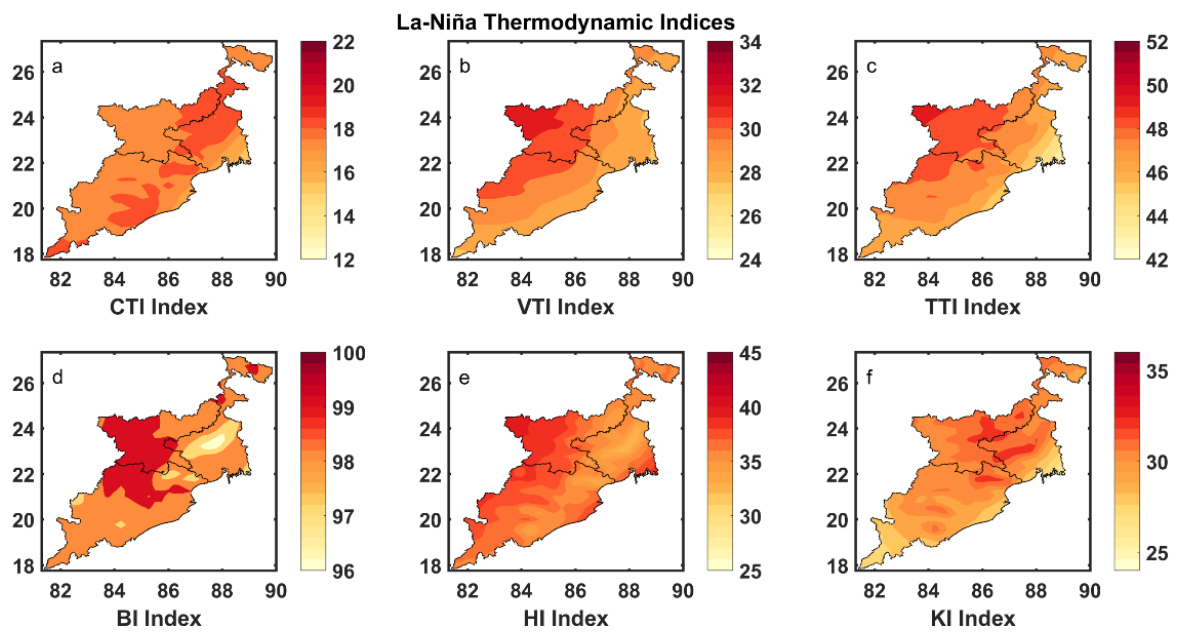


Figure 7. CTI (a), VTI (b), TTI (c), BI (d), HI (e), KI (f) variations during La-Niña years from 1998 to 2014.

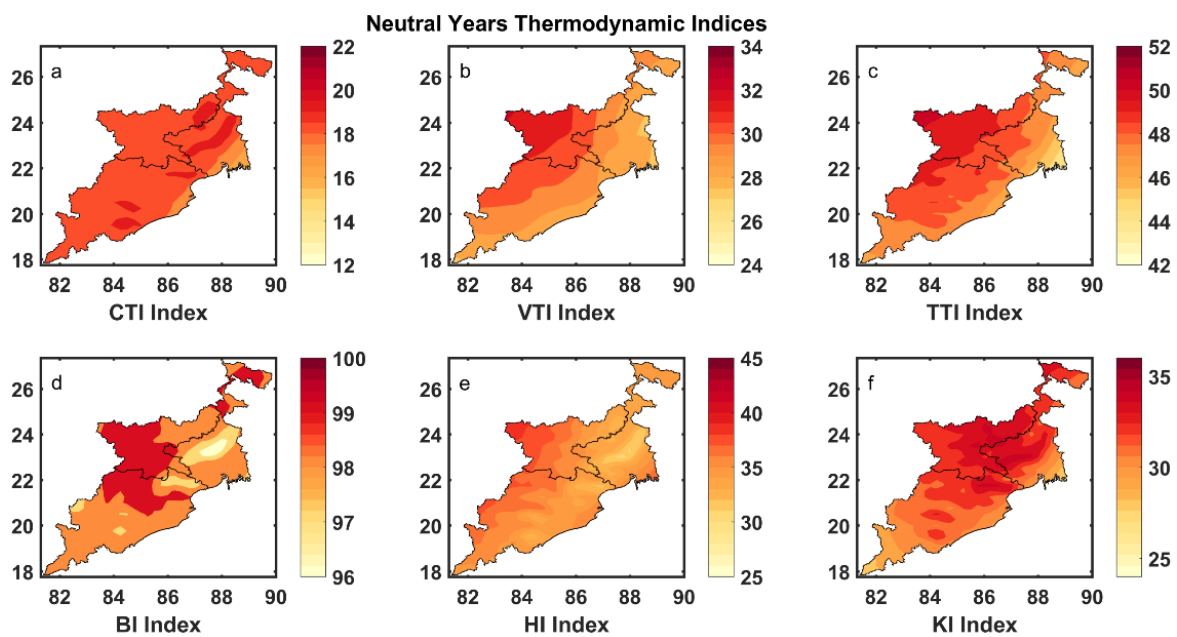


Figure 8. CTI (a), VTI (b), TTI (c), BI (d), HI (e), KI (f) variations during neutral El-Niño and La-Niña years from 1987 to 2019.

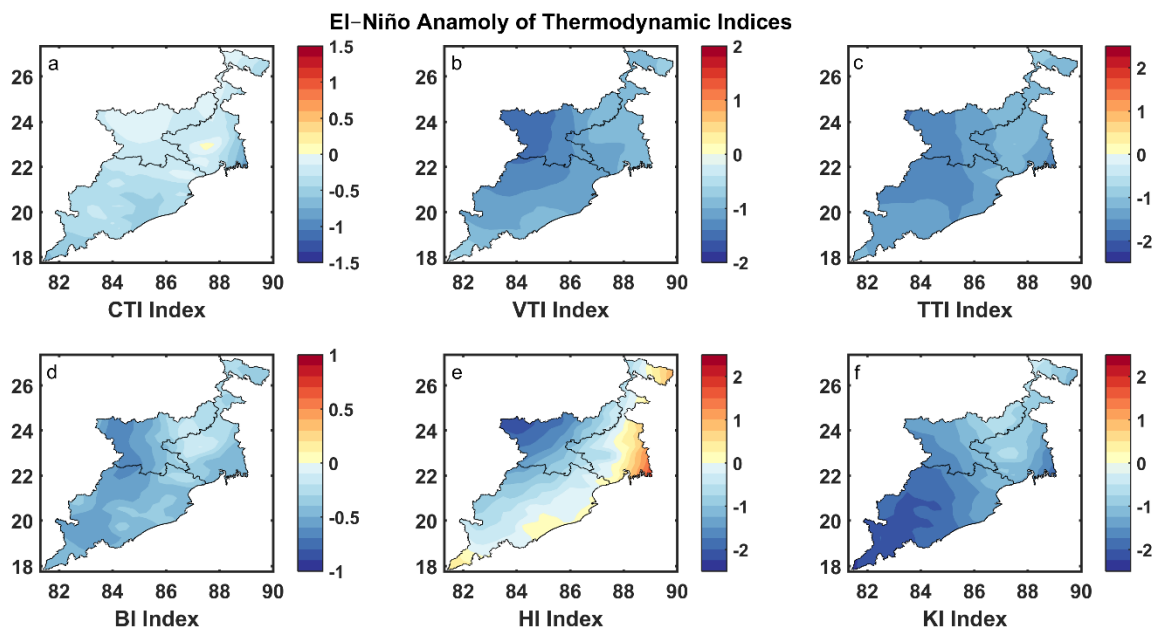


Figure 9. CTI (a), VTI (b), TTI (c), BI (d), HI (e), KI (f) anomalies during El-Niño years from 1987 to 2019.

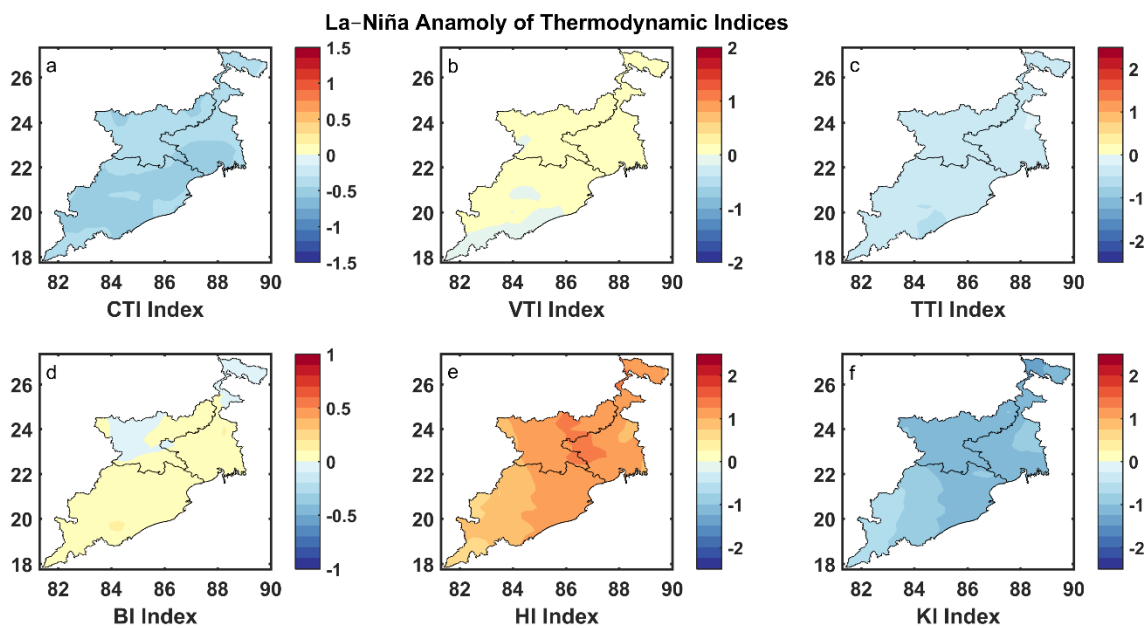


Figure 10. CTI (a), VTI (b), TTI (c), BI (d), HI (e), KI (f) anomalies during La-Niña years from 1987 to 2019.

#### 4. Summary

The results can be summarized as follows:

- The lightning FRD was higher during the El-Niño period over most of the study region. During El-Niño, the FRD anomalies were positive over parts of Odisha (southern, central, and northern), West Bengal (northern, some parts of western and eastern), and Jharkhand (central, southern, and some parts of north-eastern and western). Other regions of all three states showed negative anomalies during El-Niño. The La-Niña periods showed less FRD (negative anomalies) than the El-Niño ones.
- The precipitation changes were not significantly different during El-Niño and La-Niña periods. However, the magnitudes were slightly higher in the La-Niña periods,

suggesting a decrease in precipitation and an increase in the lightning flash rate during the El-Niño season. In contrast, the FRD decreased, and precipitation increased during the La-Niña seasons.

- During the El-Niño and La-Niña, the thermodynamic indices varied differently. The CAPE, CIN, SWEAT, VTI, TTI, BI, HI, and KI values increased, while CTI decreased during the La-Niña period. The BI values did not show significant changes, while HI values were clearly differentiated during the El-Niño and La-Niña periods.

The current research aims to assist forecasters in building climatological maps throughout multiple Indian states to understand the spatial variation of thermodynamic indices and associated lightning and rainfall activities during the El-Niño and La-Niña phases. This will aid in spotting convective occurrences and providing an early warning to the public and policymakers about the severity of the events during these phases. The findings will help researchers to better understand the pre-monsoon convective activities and associated rainfall and lightning activities over eastern India.

**Author Contributions:** R.K.S.: methodology, writing, software, and visualization; G.C.: methodology and software; N.K.V.: methodology and software; S.N.: methodology and writing; B.T.: conceptualization, writing, and supervision. All authors have read and agreed to the published version of the manuscript.

**Funding:** This research received funding from Science and Engineering Research Board (SERB), Department of Science and Technology, Govt. of India [project-funding code: DST/SERB/ECR/2017/001361].

**Institutional Review Board Statement:** Not applicable.

**Informed Consent Statement:** Not applicable.

**Data Availability Statement:** ERA5 datasets used in the study were obtained from <https://cds.climate.copernicus.eu/cdsapp#!/dataset/reanalysis-era5-land?tab=form> (accessed on 24 July 2020). The geographic location of lightning flash was obtained from the satellite Tropical Rainfall Measuring Mission with lightning imaging sensor (TRMM-LIS) for the available pre-monsoon period 1998–2014 (<https://ghrc.nsstc.nasa.gov/hydro/#/details?ds=lislip>) (accessed on 24 July 2020). TRMM/3B43 V7 L3 monthly mean rainfall data for the pre-monsoon period obtained from the Tropical Rainfall Measuring Mission satellite ([https://disc.gsfc.nasa.gov/datasets/TRMM\\_3B43\\_7/summary?keywords=TRMM](https://disc.gsfc.nasa.gov/datasets/TRMM_3B43_7/summary?keywords=TRMM)) (accessed on 24 July 2020). The details of the El-Niño and La-Niña years were collected from the National Oceanic Atmospheric Administration's Climate Prediction Center (NOAA/CPC) of the National Weather Service ([https://origin.cpc.ncep.noaa.gov/products/analysis\\_monitoring/ensostuff/ONI\\_v5.php](https://origin.cpc.ncep.noaa.gov/products/analysis_monitoring/ensostuff/ONI_v5.php)) (accessed on 24 July 2020).

**Acknowledgments:** The authors would like to acknowledge Science and Engineering Research Board (SERB), Department of Science and Technology, Govt. of India for providing the funding [project-funding code: DST/SERB/ECR/2017/001361]. The authors are also thankful to India Meteorology Department for providing the thunderstorm information for the present study. Rajesh Kumar Sahu would like to acknowledge National Institute of Technology Rourkela for providing research facilities and Manoj Hari and Venkat Sai for providing assistance in plots.

**Conflicts of Interest:** The authors declare no conflict of interest.

## References

1. NOAA Climate Staff. *El Niño and La Niña: Frequently Asked Questions*; NOAA Climate Staff: College Park, MD, USA, 2016.
2. Ahrens, C.D. *Meteorology Today: An Introduction to Weather, Climate, and the Environment*; Cengage Learning: Boston, MA, USA, 2009; ISBN 9780495555735.
3. Ju, J.; Slingo, J. The Asian summer monsoon and ENSO. *Q. J. R. Meteorol. Soc.* **1995**, *121*, 1133–1168. [[CrossRef](#)]
4. Wang, C. ENSO, Atlantic Climate Variability, and the Walker and Hadley Circulations. In *The Hadley Circulation: Present, Past and Future. Advances in Global Change Research*; Diaz, H.F., Bradley, R.S., Eds.; Springer: Dordrecht, The Netherlands, 2004; Volume 21.
5. Yuan, T.; Di, Y. Variability of lightning flash and thunderstorm over eastern China and Indonesia on ENSO time scales. In *Proceedings of the International Conference on Atmospheric Electricity, ICAE 2014, Norman, OK, USA, 15–20 June 2014*.
6. Hamid, E.Y.; Kawasaki, Z.I.; Mardiana, R. Impact of the 1997–98 El Niño event on lightning activity over Indonesia. *Geophys. Res. Lett.* **2001**, *28*, 147–150. [[CrossRef](#)]

7. Kandalgaonkar, S.S.; Kulkarni, J.R.; Tinmaker, M.I.R.; Kulkarni, M.K. Land-ocean contrasts in lightning activity over the Indian region. *Int. J. Climatol.* **2010**, *30*, 137–145. [[CrossRef](#)]
8. Kumar, P.R.; Kamra, A.K. Variability of lightning activity in South/Southeast Asia during 1997–98 and 2002–03 El Niño/La Niña events. *Atmos. Res.* **2012**, *118*, 84–102. [[CrossRef](#)]
9. Kulkarni, M.K.; Revadekar, J.V.; Verikoden, H.; Athale, S. Thunderstorm days and lightning activity in association with El Niño. *Vayu Mandal* **2015**, *41*, 39–43.
10. Tinmaker, M.I.R.; Aslam, M.Y.; Ghude, S.D.; Chate, D.M. Lightning activity with rainfall during El Niño and La Niña events over India. *Theor. Appl. Climatol.* **2017**, *130*, 391–400. [[CrossRef](#)]
11. Shinji, O.; Morimoto, T.; Kawasak, Z.-I. The Contrast of the El Niño and La Niña Events on the Convection over East Asia. 2011. Available online: [https://www.eorc.jaxa.jp/TRMM/museum/event/2ndTISC/HP/Extended%20Abstract/2P.4\\_OITA\\_Shinji\\_Rv.pdf](https://www.eorc.jaxa.jp/TRMM/museum/event/2ndTISC/HP/Extended%20Abstract/2P.4_OITA_Shinji_Rv.pdf) (accessed on 6 June 2022).
12. Ahmad, A.; Ghosh, M. Variability of lightning activity over India on ENSO time scales. *Adv. Space Res.* **2017**, *60*, 2379–2388. [[CrossRef](#)]
13. Kulkarni, M.K.; Revadekar, J.V.; Varikoden, H. About the variability in thunderstorm and rainfall activity over India and its association with El Niño and La Niña. *Nat. Hazards* **2013**, *69*, 2005–2019. [[CrossRef](#)]
14. Roy, I.; Tedeschi, R.G.; Collins, M. ENSO teleconnections to the Indian summer monsoon under changing climate. *Int. J. Climatol.* **2019**, *39*, 3031–3042. [[CrossRef](#)]
15. Saha, U.; Siingh, D.; Midya, S.K.; Singh, R.P.; Singh, A.K.; Kumar, S. Spatio-temporal variability of lightning and convective activity over South/South-East Asia with an emphasis during El Niño and La Niña. *Atmos. Res.* **2017**, *197*, 150–166. [[CrossRef](#)]
16. de Abreu, L.P.; Gonçalves, W.A.; Mattos, E.V.; Albrecht, R.I. Assessment of the total lightning flash rate density (FRD) in northeast Brazil (NEB) based on TRMM orbital data from 1998 to 2013. *Int. J. Appl. Earth Obs. Geoinf.* **2020**, *93*, 102195. [[CrossRef](#)]
17. Deierling, W.; Petersen, W.A. Total lightning activity as an indicator of updraft characteristics. *J. Geophys. Res. Atmos.* **2008**, *113*, D16210. [[CrossRef](#)]
18. Rafati, S.; Fattahi, E. Effects of Regional Thermodynamic Parameters on Lightning Flash Density as an Indicator of Convective Activity Over Southwest Iran. *Pure Appl. Geophys.* **2022**, *179*, 2011–2025. [[CrossRef](#)]
19. Mondal, U.; Panda, S.K.; Das, S.; Sharma, D. Spatio-temporal variability of lightning climatology and its association with thunderstorm indices over India. *Theor. Appl. Climatol.* **2022**, *149*, 273–289. [[CrossRef](#)]
20. Tyagi, B.; Sahu, R.K.; Vissa, N.K.; Hari, M. Reviewing the Thermodynamic Changes in the Atmosphere Associated with Pre-Monsoon Thunderstorms over Eastern and North-Eastern India. In *Extreme Natural Events—Sustainable Solutions for Developing Countries*; Unnikrishnan, A.S., Tangang, F., Durrheim, R., Eds.; Springer Nature Publications: Berlin/Heidelberg, Germany, 2022; *in press*. [[CrossRef](#)]
21. Tyagi, B.; Krishna, V.N.; Satyanarayana, A.N.V. Study of thermodynamic indices in forecasting pre-monsoon thunderstorms over Kolkata during STORM pilot phase 2006–2008. *Nat. Hazards* **2011**, *56*, 681–698. [[CrossRef](#)]
22. Madala, S.; Satyanarayana, A.N.V.; Tyagi, B. Performance evaluation of convective parameterization schemes of WRF-ARW model in the simulation of pre-monsoon thunderstorm events over Kharagpur using STORM data sets. *Int. J. Comput. Appl.* **2013**, *71*, 43–50. [[CrossRef](#)]
23. Tyagi, B.; Satyanarayana, A.N.V.; Rajvanshi, R.K.; Mandal, M. Surface energy exchanges during pre-monsoon thunderstorm activity over a tropical station Kharagpur. *Pure Appl. Geophys.* **2014**, *171*, 1445–1459. [[CrossRef](#)]
24. Tyagi, B.; Satyanarayana, A.N.V. Delineation of surface energy exchanges variations during thunderstorm and non-thunderstorm days during pre-monsoon season. *J. Atmos. Sol. Terr. Phys.* **2015**, *122*, 138–144. [[CrossRef](#)]
25. Bhardwaj, P.; Singh, O.; Kumar, D. Spatial and temporal variations in thunderstorm casualties over India. *Singap. J. Trop. Geogr.* **2017**, *38*, 293–312. [[CrossRef](#)]
26. Yadava, P.K.; Soni, M.; Verma, S.; Kumar, H.; Sharma, A.; Payra, S. The major lightning regions and associated casualties over India. *Nat. Hazards* **2020**, *110*, 217–229. [[CrossRef](#)]
27. Chaudhuri, S.; Middey, A. A composite stability index for dichotomous forecast of thunderstorms. *Theor. Appl. Climatol.* **2012**, *110*, 457–469. [[CrossRef](#)]
28. Chaudhuri, S.; Pal, J.; Middey, A.; Goswami, S. Nowcasting Bordoichila with a composite stability index. *Nat. Hazards* **2013**, *66*, 591–607. [[CrossRef](#)]
29. Samanta, S.; Tyagi, B.; Vissa, N.K.; Sahu, R.K. A new thermodynamic index for thunderstorm detection based on cloud base height and equivalent potential temperature. *J. Atmos. Sol. Terr. Phys.* **2020**, *207*, 105367. [[CrossRef](#)]
30. Tyagi, B. Surface Energy Exchanges and Thermodynamical Structure of Atmospheric Boundary Layer during Pre-Monsoon Thunderstorm Season over Two Tropical Stations. Ph.D. Dissertation, IIT Kharagpur, Kharagpur, India, 2012.
31. Haklander, A.J.; Van Delden, A. Thunderstorm predictors and their forecast skill for the Netherlands. *Atmos. Res.* **2003**, *67–68*, 273–299. [[CrossRef](#)]
32. Kunz, M. The skill of convective parameters and indices to predict isolated and severe thunderstorms. *Nat. Hazards Earth Syst. Sci.* **2007**, *7*, 327–342. [[CrossRef](#)]
33. Murugavel, P.; Pawar, S.D.; Gopalakrishnan, V. Trends of Convective Available Potential Energy over the Indian region and its effect on rainfall. *Int. J. Climatol.* **2012**, *32*, 1362–1372. [[CrossRef](#)]



34. Chakraborty, R.; Venkat Ratnam, M.; Basha, S.G. Long-term trends of instability and associated parameters over the Indian region obtained using a radiosonde network. *Atmos. Chem. Phys.* **2019**, *19*, 3687–3705. [[CrossRef](#)]
35. Sahu, R.K.; Dadich, J.; Tyagi, B.; Vissa, N.K. Trends of thermodynamic indices thresholds over two tropical stations of north-east India during pre-monsoon thunderstorms. *J. Atmos. Sol. Terr. Phys.* **2020**, *211*, 105472. [[CrossRef](#)]
36. Sahu, R.K.; Dadich, J.; Tyagi, B.; Vissa, N.K.; Singh, J. Evaluating the impact of climate change in threshold values of thermodynamic indices during pre-monsoon thunderstorm season over Eastern India. *Nat. Hazards* **2020**, *102*, 1541–1569. [[CrossRef](#)]
37. Hersbach, H.; Dee, D. ERA5 Reanalysis Is in Production. ECMWF Newsletter. 2016. Available online: <https://www.ecmwf.int/en/newsletter/147/news/era5-reanalysis-production> (accessed on 29 December 2021).
38. Christian, H.J.; Blakeslee, R.J.; Goodman, S.J.; Mach, D.A.; Stewart, M.F.; Buechler, D.E.; Koshak, W.J.; Hall, J.M.; Boeck, W.L.; Driscoll, K.T.; et al. The Lightning Imaging Sensor. In Proceedings of the 11th International Conference on Atmospheric Electricity, Guntersville, AL, USA, 7–11 June 1999.
39. Boccippio, D.J.; Koshak, W.J.; Blakeslee, R.J. Performance assessment of the optical transient detector and lightning imaging sensor. Part I: Predicted diurnal variability. *J. Atmos. Ocean. Technol.* **2002**, *19*, 1318–1332. [[CrossRef](#)]
40. Cecil, D.J.; Buechler, D.E.; Blakeslee, R.J. Gridded lightning climatology from TRMM-LIS and OTD: Dataset description. *Atmos. Res.* **2014**, *135–136*, 404–414. [[CrossRef](#)]
41. Williams, E.; Rothkin, K.; Stevenson, D.; Boccippio, D. Global lightning variations caused by changes in thunderstorm flash rate and by changes in the number of thunderstorms. *J. Appl. Meteorol.* **2000**, *39*, 2223–2230. [[CrossRef](#)]
42. Bond, D.W.; Steiger, S.; Zhang, R.; Tie, X.; Orville, R.E. The importance of NO<sub>x</sub> production by lightning in the tropics. *Atmos. Environ.* **2002**, *36*, 1509–1519. [[CrossRef](#)]
43. Anandh, P.C.; Vissa, N.K. Role of synoptic-scale circulations, mechanisms, and precursors during extreme rainfall events over the Southern Indian Peninsula. *Meteorol. Atmos. Phys.* **2022**, *134*, 27. [[CrossRef](#)]
44. Sahu, R.K.; Tyagi, B. Spatial variation of thermodynamic indices over north-east India during pre-monsoon thunderstorm season. *J. Atmos. Sol. Terr. Phys.* **2022**, *232*, 105868. [[CrossRef](#)]
45. Sahu, R.K.; Tyagi, B.; Vissa, N.K.; Mohapatra, M. Pre-monsoon thunderstorm season climatology of Convective Available Potential Energy (CAPE) and Convective Inhibition (CIN) over Eastern India. *MAUSAM* **2022**, *73*, 565–586. [[CrossRef](#)]